RECyT
Year 27 / Nº 43 / 2025 /
DOI: https://doi.org/10.36995/j.recyt.2025.43.002

Wettability Device for Electronic Solder Alloys Using the Sessile Drop Method

Dispositivo de Humectabilidad para Aleaciones de Soldadura Electrónica Utilizando el Método de Gota Sésil

Dispositivo de Molhabilidade para Ligas e Soldagem Eletrônica Usando o Método de Gota Séssil

Héricles R. O., Souza[1, *]; André C. C., Maciel[1]; Ariadne C. B., Farias[1]; Nádia S., Cosmo[1]; Maria A. P. S., Silva[1]

1- Instituto de Tecnologia. Universidade Federal do Pará. Belém, Pará, Brasil.
* E-mail: hericlesoliveira.ho@gmail.com

Received: 25/11/2023; Accepted: 20/11/2024

Abstract
In 2003, the RoHS (Restriction of Certain Hazardous Substances) Directive emerged in the European Union to restrict hazardous substances in electronics, prompting the search for alternatives to lead-based solder due to health concerns related to its toxicity. Soft solder, working at low temperatures (up to 450 °C), is essential in heat-sensitive electronic components. With the evolution of smart electronics, wettability (the ability of liquids to spread on solid surfaces) has become critical for the integration, power, miniaturization, and flexibility of electronics. However, the scarcity of affordable devices to test wettability limits research in this promising field. Addressing this need, an affordable device, costing around US$ 30.00, was developed to measure the wettability of low-temperature alloys. The construction was carried out by planning its structure and geometry through parametric 3D CAD (Computer Aided Design) modeling software. Then, the components were manufactured and assembled to conduct a wettability test. The device provided material dripping onto copper substrates, eliminating the need for prior contact. After six tests, the results revealed contact angles ranging from 139.08° to 147.93°, indicating partial wettability and low adhesion due to material drop caused by air resistance. This functional and affordable device can drive studies in the field, promoting research on lead-free solder and new materials for electronic components.

Keywords: lead-free, device development, wettability, sessile drop, electronic components.

Resumen
La Directiva RoHS (Restriction of Certain Hazardous Substances) surgió en la Unión Europea en el 2003 para restringir sustancias peligrosas en dispositivos electrónicos, impulsando la búsqueda de alternativas a la soldadura a base de plomo debido a preocupaciones de salud relacionadas con la toxicidad del plomo. La soldadura suave, al trabajar a bajas temperaturas (hasta 450 °C), es esencial en componentes electrónicos sensibles al calor. Con la evolución de la electrónica inteligente, la mojabilidad (la capacidad de los líquidos para extenderse sobre superficies sólidas) se ha vuelto crítica para la integración, potencia, miniaturización y flexibilidad de la electrónica. Sin embargo, la escasez de dispositivos asequibles para probar la humectabilidad limita la investigación en este campo prometedor. En respuesta a esta necesidad, se desarrolló un dispositivo asequible, con un costo de alrededor de US$ 30.00, para medir la humectabilidad de aleaciones de baja temperatura. La construcción se llevó a cabo planificando su estructura y geometría a través de un software modelador CAD (computer-aided design) paramétrico en 3D. Luego, los componentes se fabricaron y ensamblaron con el objetivo de realizar una prueba de mojabilidad. El dispositivo proporcionó goteo de material sobre sustratos de cobre, eliminando la necesidad de contacto previo. Después de seis pruebas, los resultados revelaron ángulos de contacto que oscilan entre 139,08° y 147,93°, indicando una mojabilidad parcial y baja adherencia debido a la caída del material causada por la resistencia del aire. Este dispositivo funcional y asequible puede impulsar estudios en el área, fomentando la investigación sobre soldadura sin plomo y nuevos materiales para componentes electrónicos.

Palabras claves: sin plomo, desarrollo de dispositivo, humectabilidad, gota sésil, componente electrónico.

Resumo
Em 2003, a Diretiva RoHS (Restriction of Certain Hazardous Substances) surgiu na União Europeia para restringir substâncias perigosas em eletrônicos, gerando a busca por alternativas à solda à base de chumbo devido a preocupações de saúde por conta da toxicidade do chumbo. A solda branda, por trabalhar em baixas temperaturas (até 450 °C), é essencial em componentes eletrônicos sensíveis ao calor. Com a evolução dos eletrônicos inteligentes, a molhabilidade (a capacidade de líquidos se espalharem em superfícies sólidas) tornou-se crítica para integração, potência, miniaturização e flexibilidade de eletrônicos. Entretanto, a escassez de dispositivos

acessíveis para testar a molhabilidade limita a pesquisa nesse campo promissor. Visando essa necessidade, um dispositivo acessível, custando cerca de US$ 30.00, foi desenvolvido para medir a molhabilidade de ligas de baixa temperatura. A construção foi feita a partir do planejamento de sua estrutura e geometria através de um software modelador CAD (computer-aided design) paramétrico em 3D, em seguida os componentes foram fabricados e montados com o objetivo da realização de um ensaio de molhabilidade, assim o dispositivo proporcionou o gotejamento do material em substratos de cobre, eliminando a necessidade de contato prévio. Após seis ensaios, os resultados revelaram ângulos de contato variando de 139,08° a 147,93°, apresentando molhabilidade parcial e baixa aderência por conta da queda do material devido à resistência do ar. Esse dispositivo funcional e acessível pode impulsionar estudos na área, promovendo pesquisas sobre solda branda sem chumbo e novos materiais para componentes eletrônicos.

Palavras-chave: livre de chumbo, desenvolvimento de dispositivo, molhabilidade, gota séssil, componentes eletrônicos.

1. Introduction

The United Nations (UN) has a clear position on lead (Pb): it is a toxic metal and can cause serious health problems. Anthropogenic activities, including industrialization, urbanization and mining have resulted in the redistribution of lead from the Earth's crust to the soil and the environment (THOMAS *et al*., 2022). "Although many countries have systematically banned or restricted its application, lead pollution has become a public health problem due to its non-biodegradable nature" (NIU *et al*., 2023). In 2003, the RoHS (Restriction of Certain Hazardous Substances) limited the use of certain hazardous substances in electrical and electronic equipment in EU members and disclosed a mechanism for additional restrictions in the future (PECHT *et al*., 2016). The RoHS originally came into effect on July 1, 2006, and later in 2011, the directive was modernized as RoHS-2. This provided deadlines for some exempt applications. It also mentioned the specific reasons for some exemptions that were essential to maintain. In 2015, the directive was revised again and further restricted some substances in electrical and electronic equipment. However, lead has proven to be hazardous to human health and the environment (PATIL and DABADE, 2019). From contact, lead has a half-life of about 30 days in the blood, after which it diffuses into soft tissues such as the kidneys, brain, and liver. Then, it is distributed to bones, teeth, and hair as lead phosphate (ENGWA *et al*., 2019). In the last 10 years, studies have shown detrimental effects on the environment and human health, with the use of many materials, including lead, being restricted and prohibited by the WEEE (Waste Electrical and Electronic Equipment) (CHENG *et al*., 2017). Still, according to Pecht *et al*. (2016), electronics manufacturers associated with excluded and exempt products often seek to preserve the use of lead-based parts and assembly processes, mainly due to the concerns regarding the long-term reliability of solder joints.

In electronics, soft soldering is a term commonly used to refer to low-temperature soldering, generally below 450°C, which is ideal for heat-sensitive electronic components, as it prevents damage to them. Thus, due to low cost, lower melting temperature, excellent mechanical and thermal properties, adequate wettability behavior and eutectic composition, Sn-Pb solders were widely used (JAFFERY *et al*., 2022). However, manufacturers have sought a new generation of lead-free solders, called Lead Free, to replace Sb-Pb solders as an alternative to this problem (ZHOU *et al*., 2023).

Liu *et al*. (2016) says that wettability is the ability of a liquid to spread over a solid surface and is measured by the contact angle. When the contact angle (θ) is small (less than 90°), the liquid tends to spread more, indicating high wettability. When the angle is large (greater than 90°) and wettability is low, the liquid tends to form droplets. According to Cosmo *et al*. (2022), wettability is an essential characteristic of the material to define weldability properties, especially in industries that use soft welding, as there is no casting between the filler alloy and the substrate. In recent years, the focus of studies about wettability testing has increased. This is associated with the use of new materials driven by the development of intelligent electronic equipment designed for high integration, power, miniaturization and folding (Kuang *et al*., 2022). Thus, due to the high cost and limited availability of the devices necessary to perform the wettability test, access to this technology is unfeasible in many places, which can hinder the development of promising research in this area. One of the most commonly used methods for analyzing the contact angle is the direct measurement of the tangent at the three-phase contact point using the sessile drop method (Figure 1) (HEBBAR *et al*., 2017).

Figure 1. Diagram of contact angle (θ), external contact angle (θ_{ext}), interfacial tensions between solid-liquid (γ_{SL}), solid-vapor (γ_{SV}) and liquid-vapor (γ_{LV}) interfaces.

In Young's equation, the surface is considered ideal (i.e., flat, non-reactive, homogeneous, and non-porous) (Ebrahim *et al.*, 2021). In the present work, it is assumed that the surface under study is ideal. These ideal conditions serve as a reference for understanding the behavior of real surfaces, facilitating the development and optimization of materials and coatings in various practical applications in science and engineering. The relationship for the contact angle was defined by physicist Thomas Young (1773-1829) and is expressed in Equation 1 below:

$$cos\, cos\,(\theta) = \frac{\gamma_{SV} - \gamma_{SL}}{\gamma_{LV}} \quad (1)$$

γ_{SV} represents the surface energy between the solid and vapor (or air), while γ_{SL} denotes the surface energy between the solid and liquid. Additionally, γ_{LV} indicates the surface energy between the liquid and vapor (or air). The contact angle formed between the solid surface and the liquid is represented by θ. θ_{ext} refers to the external contact angle formed between the liquid surface and the vapor (or air). For contrast purposes, in some images, it is preferable to measure the θ_{ext} using the optical method of the sessile droplet so that it is possible to determine the θ (Equation 2).

$$\theta = 180° - \theta_{ext} \quad (2)$$

For Cosmo *et al*. (2022), this method consists of placing the material with the lowest melting point on the prepared surface of the solid substrate and heating the substrate until the material melts. However, some variations of this procedure are also used, such as dripping the material with a lower melting point onto the solid substrate at the desired temperature and avoiding prior contact with the materials, carried out by Sehirli *et al*. (2022).

The term *lead-free* refers to products or materials that do not contain lead. “For a long time, tin-lead alloys have been the main soldering materials in the field of electronic welding because of their good electrical conductivity, mechanical properties, and low cost” (GAN and NGAN, 2018; JIANG *et al*., 2019). The most commonly used alloy for microelectronics soldering is tin-lead eutectic, which is composed of approximately 63% Sn and 37% Pb (ŠURYOVÁ *et al*., 2020). Its melting point is around 183 °C, which prevents overheating of soldered electronic components (WERNICKI, 2023). However, due to restrictions on the use of this toxic metal, researchers around the world have carried out many studies on lead-free solder alloys. Tehrefore, tin-based (Sn-based) alloys are considered the most promising candidates to replace the traditional Sn-Pb solder alloy (LI Y. *et al*., 2020).

Two candidate alloys are Sn-2wt.%Sb, tested by Dias *et al*. (2015) and Rocha *et al*. (2018), and Sn-5.5wt.%Sb tested by Cosmo *et al*. (2022). The composition of these alloys has better resistance to room temperature, ductility, and greater microstructural stability when compared to Sn-Pb system alloys. Although the commercial Sn-37wt.%Pb alloy presented smaller angles than those of lead-free alloys, the difference is not significant, suggesting that Sb-containing alloys are potential substitutes for commercial lead-based alloys (COSMO *et al*., 2022).

Therefore, aiming to meet the study needs, the general objective of this work is the sizing, development, verification, and presentation of the costs of manufacturing a wettability analysis device for alloys up to 400 ºC. This device will use a variation of the sessile drop method that takes into account the free fall of the material. The development of this device aims to provide savings in the device purchasing value to enable future research in wettability with alternative lead-free alloys.

2. Materials and Methods

Various materials were used during the development of the device. Some of these materials are part of the device, while others helped in its creation. The distinction between these materials is important since the costs of developing the device will only include the materials and components that comprise it.

2.1. Device and Auxiliary Materials

Most of the materials that comprise the device were purchased, but some, such as the tiltable stand and the substrate platform, were reused (Figure 2).

Figure 2. Materials that integrate the wettability device.

Next, Figure 3 shows the auxiliary materials that belong to the laboratory where the device was developed, and for this reason, their purchasing values will not be counted.

Figure 3. Materials used during the development of the wettability device.

2.2. Development Methodology

2.2.1. Making the Device Support

Some of the requirements for selecting and manufacturing the bases of this wettability device are the type of material, inclination, stability, size, and mobility. Taking these aspects into account, two components within the laboratory that met these characteristics were unusable, but they were reused for the development of the device. Both components belonged to damaged laboratory microscopes. One of these was the adjustable base made of aluminum, which has a melting point of 660 °C and was of a suitable size for mobility. Moreover, the substrate structure has an adjustable height, which facilitates the determination of the height at which the liquid drop falls. Therefore, the substrate platform was attached to the front of the adjustable stand and fixed by screws, forming a single structure. Furthermore, some holes were made in the adjustable base for securing screws to the ceramic piece and substrate platform and for passing the power cable, shown in the red circles in Figure 4.

Figure 4. Union of the manufactured support.

Inserting the power cable into the back of the apparatus prevents the wires from being affected by the heat of the test and ensures they remain firm with the help of the clamp.

2.2.2. Production of the Ceramic Piece and its Components

The objective of the ceramic part is to concentrate the heat emitted from the test in itself, preventing the heat from being dissipated from the system. Therefore, to obtain the model of the part, © FreeCAD (3D parametric CAD—computer-aided design and modeling software) in Figure 5a was used. Through the design of the part, additive manufacturing was used to obtain a 3D printed mold, thus making it possible to develop the established dimensions and desired geometry. Figure 5b shows the mold model developed and printed in 3D.

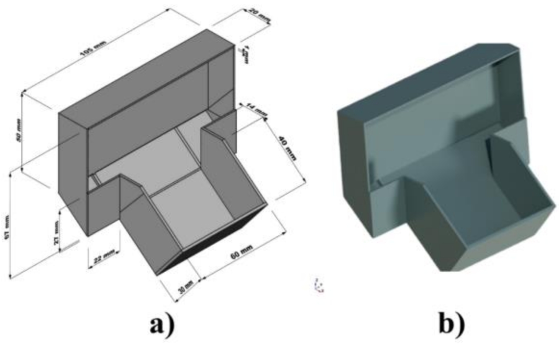

Figure 5. a) Mold model design and b) 3D mold printing.

In the next stage, the composition materials of the ceramic piece were used to obtain the final mass of the piece. To obtain a piece that was highly resistant to high temperatures, the recommendation on the packaging of the refractory mass was followed. A proportion of 5:1:1 (refractory: cement: sand) was recommended for intermediate mass, consistent Pivinskii's (2021) findings on the reduction of mixtures to increase resistance to high temperatures. However, clay was also included in the intermediate mass in a ratio of 2:1 (intermediate-mass: clay), as it can be molded easily due to its high plasticity, presenting structural resistance after firing at high temperatures (ALMEIDA *et al.*, 2015). Furthermore, after obtaining the final mass, a ratio of 1:5 (water: final mass) was used to obtain the final mixture. The next step consisted of depositing the final mixture into the mold and waiting 24 hours for pre-curing. After that, the piece was removed from the mold and placed in an oven (Figure 6a) at 150 °C for 30 minutes to bake and dehumidify the piece. Then, with the piece prepared, roughing was carried out in the frontal region to open a channel (Figure 6b), this being the place where the resistance that will emit heat will be deposited. In addition, holes were made for the screws that will fix the piece to the support. Finally, the aluminum sheet was made to suspend the metal that will be cast, covering the front part of the ceramic piece (Figures 6c, 6d, and 6e). The complete production is shown in Figure 6.

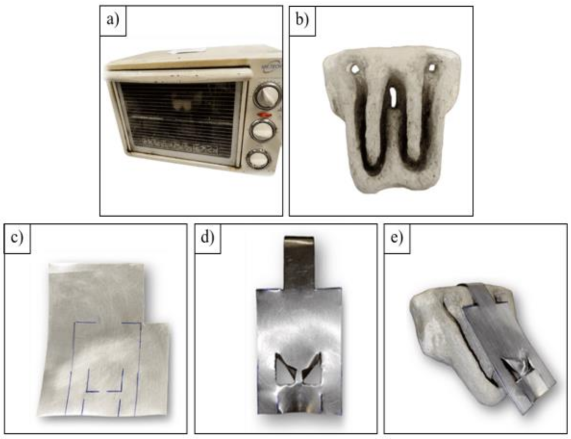

Figure 6. a) ceramic piece in the oven; b) front roughing; c) drawing for aluminum sheet cutting; d) cut aluminum sheet, and e) final result.

The resistance channel is relatively deep. Therefore, the aluminum sheet will not come into direct contact with the resistance, thus avoiding a short circuit in the system.

2.2.3. Device Assembly

With all the device components made and prepared, the next step consisted of assembling the device, as shown below:

1) Initially, the power cables were inserted into the holes designed to support the device, and they were tied to the base with a cable so that they would not come loose.

2) The electrical resistance was fitted into the channel (in the lower front part of the piece) and its two ends were connected to each of the screws (in the upper front part of the part ends). This connection aims to pass electrical current through the resistance, thus heating it due to the Joule effect, to induce heat in the experiment.

3) The ceramic piece was attached to the base and fixed using a screw and a nut (in the middle of the piece);

4) The stripped ends of the power cable were wrapped around the two screws (on the upper back of the ends of the piece) and were firmly tightened between the nuts and washers;

5) The aluminum sheet overlaps the ceramic piece (on the front of the piece) so that it is heated by the heat from the electrical resistance through conduction.

6) Finally, the current controller was coupled to the device's power cable so that it was possible to control the power of the electrical resistance. Therefore, the assembled device can be seen in Figure 7, which displays several viewing perspectives.

Figure 7. Display of the developed wettability device (without aluminum sheet) from various perspectives.

In Figure 7 above, the device is shown without the aluminum sheet, allowing for an analysis of its interior. As noted, the device was rigid, stable, and functional, ready to perform the six planned tests. However, the copper substrates and the specimens to be tested still needed to be prepared.

2.2.4. Preparation of Copper Substrates and Test Specimens

Considering the importance of the substrate parameters for carrying out the test, the surface must come close to the ideal model proposed by Young, which must be clean and as smooth as possible. Thus, Figure 8 shows the steps that were followed to obtain the copper substrates and the alloy test specimens used for the test.

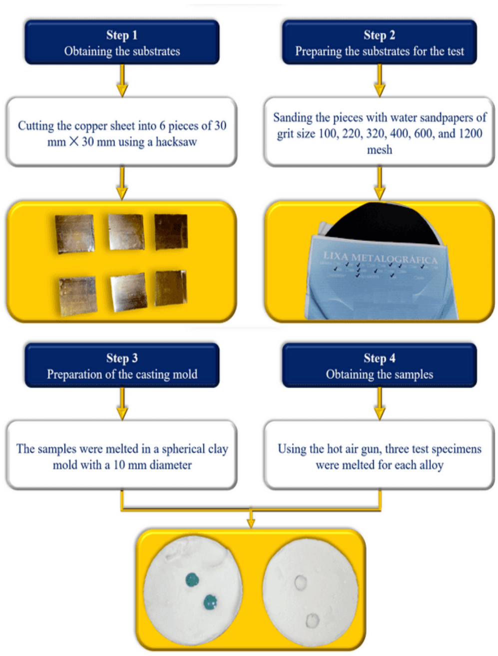

Figure 8. Steps for obtaining and preparing copper substrates for testing and test specimens.

As mentioned before, two alloys will be used to compare the test angles, Sn-5.5wt.%Sb and Sn-37wt.%Pb, with three test specimens for each alloy.

2.2.5. Carrying out the Wettability Test

After assembling the device and preparing the copper substrates and test specimens, it was possible to carry out wettability tests using the developed device. Thus, the test followed these steps:

1) Firstly, because one of the alloys contains lead in its composition, PPE (Personal Protective Equipment) such as masks, gloves, boots, and glasses were used to avoid contact with the toxic metal.

2) Each of the six specimens to be tested was placed on the aluminum sheet, one for each test. Then, the sheet was superimposed on the ceramic piece to transmit heat to the specimen.

3) The copper substrate was leveled at approximately 180° with the aid of the spirit level so that there was no difference caused by unevenness. In addition, the distance of the lower edge of the aluminum sheet was adjusted to 1 cm to try to prevent the liquid drop from being significantly affected by the effect of air resistance and from solidifying during the fall.

4) The pyrometer was configured and fixed on a tripod and positioned to measure the temperature of the contact line between the test piece and the aluminum sheet.

5) Since there is still no place for thermal insulation of the device, the test environment was controlled to avoid air currents near the device during the experiment, thus avoiding changes in results due to temperature variation.

6) The device's power cable was connected to the current controller to control the resistance power in a 110 V socket.

7) With the current controller, the resistance power was increased, thus increasing the heat emitted to the aluminum sheet, which consequently increased the temperature of the test piece.

8)The drop of the test piece on the copper substrate had a distance of 1 cm and was recorded by a cell phone camera to observe the way the drop fell and its adhesion to the copper substrate. Moreover, the aluminum sheet was readapted not only to heat the metal to be melted but also to heat the copper substrate by conduction, thus facilitating the union of the droplet with the substrate. Figure 9 shows a schematic of the device and the droplet as it falls onto the substrate.

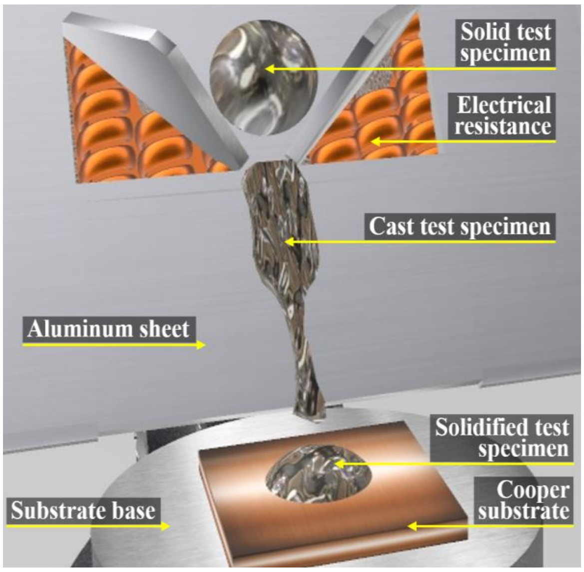

Figure 9. Schematic of the device showing the droplet falling onto the substrate.

Finally, measurements of the external contact angles (θ_{ext}) were carried out using the optical sessile droplet method. Three stereoscope images of the test specimen were taken to determine the average of the angles, standard deviations, and coefficients of variation, as calculated by Equations 3, 4, and 5, respectively.

$$\underline{\theta} = \frac{\sum \quad \theta_i}{n} \quad (3)$$

$$s = \sqrt[2]{\left(\frac{\sum \quad (\theta_i - \underline{\theta})^2}{n-1}\right)} \quad (4)$$

$$CV = \frac{s}{\underline{\theta}} \times 100\% \quad (5)$$

Hence, it is possible to check through these equations the average reliability of the contact angle measured, since the standard deviation and coefficient of variation are measures that allow the analysis of data dispersion. That is, they are used to measure the average dispersion around the average arithmetic.

3. Results

3.1. Measurement of the Developed Wettability Device

The equipment weighs approximately 1.2 kg and its dimensions are 34.0 cm in height and 8.0 cm in width. It has a tilt of 45, and the liquid material is suspended at a distance of 1.0 cm from the copper platform (which can be altered by varying the height of the copper substrate). The aluminum sheet was changed twice during the tests, meaning one sheet for every three tests of each alloy. The device is shown in Figure 10.

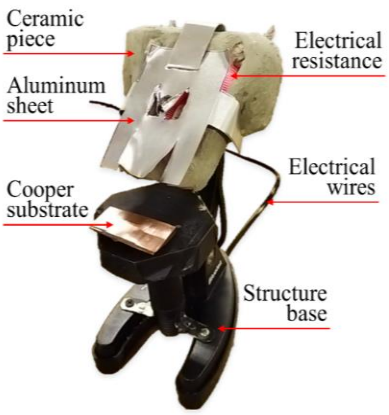

Figure 10. The developed wettability device.

To carry out the tests, it was necessary to wait for the copper substrates to reach a temperature of 50 °C so that a good union between the metals could occur. Additionally, using the Optical Pyrometer, it was noted that the maximum temperature the device reaches is 650 °C. However, for safety reasons, the device will be operated up to a temperature of 400°C, representing the ideal temperature for the project. Hence, the burning of the electrical resistance is avoided. The sequence illustrates the transformation of a solid droplet into a liquid flowing over the heated aluminum foil (Figure 11).

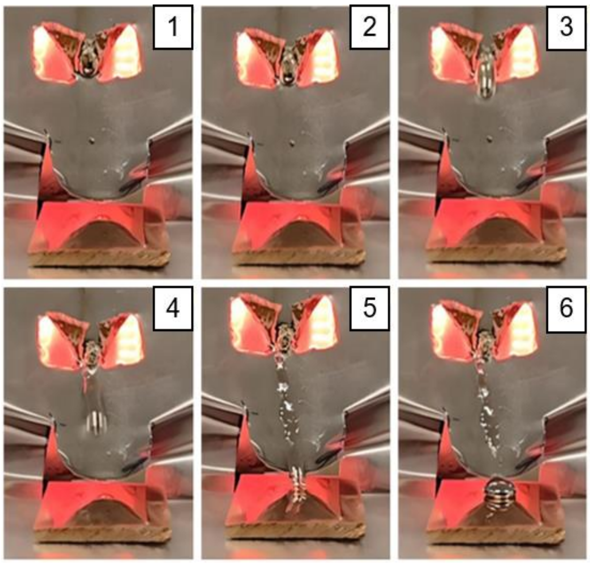

Figure 11. Recording the droplet falling on the copper substrate.

In the first stage, the solid droplet is at the top, maintaining its shape. In the second, liquefaction begins, making the surface shiny. In the third stage, the droplet starts to descend due to gravity, elongating as it falls. In the fourth, it is midway down, with the liquid flowing to the bottom. In the fifth stage, the droplet reaches the tip of the fall and is about to detach. Finally, in the sixth stage, the droplet is released, and it is deposited onto the copper substrate, spreading out upon contact.

3.2. Measurements of the Contact Angle and External Contact Angle

After measuring the wettability device and validating it after carrying out the tests, the test specimens were identified and grouped as shown in Figure 12.

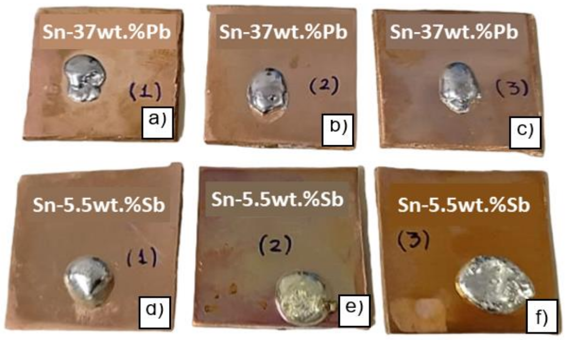

Figure 12. a), b), c) 1st, 2nd and 3rd test specimen of lead alloy; d), e), f) 1st, 2nd and 3rd test specimen of lead-free alloy.

During the testing of Sn-37wt.%Pb alloy specimens, it was observed that the droplets tended to form with one end wetting the substrate in a circular shape, while the other end displayed irregularities. This occurs as the droplet falls, since the contact area between the aluminum plate and the liquid droplet decreases, reducing heat transfer between them. This results in the droplet solidifying in midair due to air resistance. Additionally, similar characteristics were observed during testing of the Sn-5.5wt.%Sb alloy, as it has a liquidus-to-solidus temperature difference of only 2 °C. The external contact angles of both alloys showed partial wettability on the copper substrates and were subsequently measured using the ImageView software in the stereoscope. An example of the measurement is shown in Figure 13.

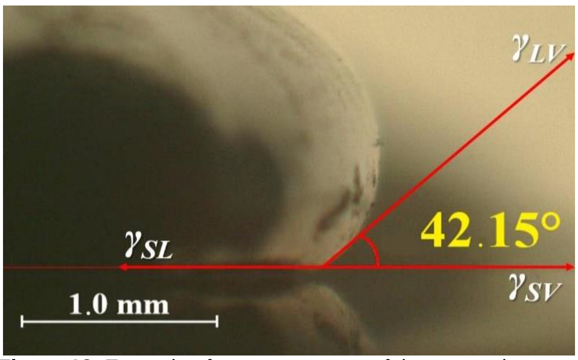

Figure 13. Example of a measurement of the external contact angle (θ_{ext}) of test specimens.

Furthermore, to maintain stability when taking images with the stereoscope, the specimens were attached to a support base. Each of the two alloys was tested three times, with three external contact angles measured for each specimen. Table 1 shows the contact angles obtained for the three Sn-37wt.%Pb alloy specimens (Equation 2), as well as their averages, standard deviations, and coefficients of variation.

Table 1. Contact angles obtained from the three test specimens of the Sn-37wt.%Sb alloy.

Test Specimen	Contact angle 1, θ_1 (°)	Contact angle 2, θ_2 (°)	Contact angle 3, θ_3 (°)	Average, $\underline{\theta}$ (°)	Standard deviation, s	Coefficient of variation, CV (%)
1	137.85	139.95	140.60	139.47	1.87	3.49
2	142.57	143.19	146.16	143.97	2.23	4.97
3	144.84	146.85	147.82	146.50	1.94	3.75

Thus, it can be observed that the maximum values of standard deviation and coefficient of variation are 2.23 and 4.97%, respectively. The same procedure was then performed for the three Sn-5.5wt.%Sb alloy specimens shown in Table 2, which presents the obtained contact angles, as well as their averages, standard deviations, and coefficients of variation.

Table 2. Contact angles obtained from the three test specimens of the Sn-5.5wt.%Sb alloy.

Test Specimen	Contact angle 1, θ_1 (°)	Contact angle 2, θ_2 (°)	Contact angle 3, θ_3 (°)	Average, $\underline{\theta}$ (°)	Standard deviation, s	Coefficient of variation, CV (%)
1	143.34	145.78	146.94	145.35	2.34	1.61
2	146.91	147.38	149.51	147.93	1.61	1.09
3	137.52	139.78	139.95	139.08	1.82	1.31

Therefore, the maximum values of standard deviation and coefficient of variation are 2.34 and 1.61%, respectively. The higher coefficient of variation (CV) values of 4.97% and 1.61% indicate low variability relative to the mean, suggesting that both samples have consistent data with little dispersion. Hence, the average contact angles obtained in Tables 1 and 2 are plotted in Graph 1.

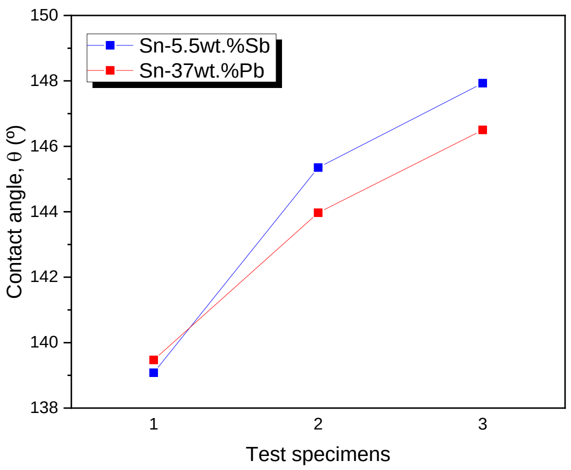

Graph 1. Average contact angles obtained from test specimens of Sn-37wt.%Pb and Sn-5.5wt.%Sb alloys.

From the graph, it can be observed that the wettability of the Sn-37%Pb alloy is better than that of the Sn-5.5%Sb alloy, as it showed lower contact angles in specimens 2 and 3, with a difference of almost 1% for each of these specimens. However, in specimen 1, the Sn-5.5%Sb alloy presented a contact angle 0.27% lower than that of the commercial lead alloy. Additionally, this observation is similar to the findings in the study by Cosmo *et al*. (2022). In that study, one out of four tested specimens also showed a lower contact angle for the Sn-5.5%Sb alloy than the commercial lead alloy, further highlighting Tin-Antimony as a promising material for lead-free alloys. Furthermore, it was found that the contact angles of the specimens in this study are approximately 7.9% lower than those reported by Cosmo *et al*. (2022). This difference can be attributed to the material falling onto the solid substrate due to gravity, which increases spreading and decreases the contact angles, an effect that did not occur in Cosmo *et al*. (2022) due to their use of the conventional sessile drop method. In contrast, some specimens in Figure 12 detached easily, which is an indication of non-adhesion as a result of insufficient heat transfer between the materials. In this case, both the copper substrate was not at the ideal temperature to create adhesion with the drop, and the drop itself lost heat during its fall, thereby preventing intermetallic compound formation for a strong bond.

3.3. Development Cost of the Device

The device was developed with the help of some materials and components already existing in the laboratory, but others were acquired for the project. Therefore, only the materials that make up the device will be included in the cost calculation. Hence, such materials and their purchasing values are shown in Table 3.

Table 3. Cost of the developed wettability device.

COMPONENTS / MATERIALS	UNITS	PRICE
500 g of clay	1	US$ 1.50
500 g of cement	1	US$ 0.10
500 g refractory dough	1	US$ 0.28
Nylon cable tie	1	US$ 0.03
2 m power cable	1	US$ 5.65
Current controller	1	US$ 9.79
Aluminum sheet 0.4 mm x 20 cm x 1 m	1	US$ 3.40
Bubble level	1	US$ 3.33
Screws, nuts, and washers 3/16" x 3/4"	2	US$ 3.39
Electrical resistance 1000 W	1	US$ 2.00
		TOTAL
		US$ 29.47

Thus, the developed device was able to perform the 6 planned tests without any issues related to functionality or durability. However, due to residue formed along the path followed by the droplet, the aluminum sheet used must be sanded or replaced when different materials are tested. The average cost of a wettability measurement device can vary considerably, depending on its precision and functionalities. In general, the price of basic wettability measurement equipment can range from about US$ 20,000 to US$ 50,000. Compared to these commercially available devices, the developed device, costing less than US$ 30.00, lacks features such as a high-resolution camera, thermal insulation, or real-time data acquisition. However, the results it produced were of great value for the research.

4. Conclusions

A small-sized and low-cost device was successfully developed, showing promise in terms of accessibility and portability, although it may lack some functionalities compared to market devices. Nevertheless, it proved to be valuable for research, undergoing tests with Sn-37wt.% Pb and Sn-5.5wt.%Sb alloys. In these experiments, patterns and trends in the wettability properties of the mentioned alloys were identified. Early solidification of sessile drops due to heat loss during the fall resulted in different wettability modes at the ends, suggesting the potential for process improvement by reducing substrate roughness or shortening the fall distance. Measurement and data processing procedures were accurate and reliable, with wettability angles calculated based on Young's equation and using the contact angle measurement technique. The values of mean, standard deviation, and coefficient of variation were consistent, indicating reliable results, and the understanding of the wettability behavior of lead-free alloys provides valuable insights for the development of new materials. This can lead to the creation of more efficient, durable, and environmentally friendly alloys for use in electronic components. From the promising results obtained in the wettability test, there is an indication that these alloys may meet environmental and joint reliability requirements, contributing to regulatory compliance. The device was effective in investigating the interaction between low-melting alloys and a copper substrate, especially in the analysis of material drop due to gravity. This resulted in an increase in spreading and contact angles but a decrease in joint adhesion, without the formation of intermetallic compounds between the materials. This study serves as a stimulus for future improvements and further research in the academic field, with the potential to significantly contribute to advancing knowledge about the wettability behavior of low-melting alloys.

5. References

Almeida, P. H. S., Franco, J. de M., & Tavares, C. R. G. (2015). Influência do tipo de argila no processo de solidificação/estabilização de lodo têxtil. *Cerâmica*, *61*(357), 137–144. https://doi.org/10.1590/0366-69132015613571870

Cheng, S., Huang, C.-M., & Pecht, M. (2017). A review of lead-free solders for electronics applications. *Microelectronics Reliability*, *75*, 77–95. https://doi.org/https://doi.org/10.1016/j.microrel.2017.06.016

Cosmo, N. S., Brabo, C. A. da S., Mesquita, S. Q., Costa, T. A. P. de S., da Rocha, O. F. L., & da Silva, M. A. P. de S. (2022). Análise Comparativa do Ângulo de Molhabilidade em uma Liga Livre de Chumbo Sn-2%Sb / Comparative Analysis of the Wetting Angle in a Lead-free Sn-2.0wt%Sb Alloy. *Brazilian Journal of Development*, *8*(2), 13655–13666. https://doi.org/10.34117/bjdv8n2-343

Dias, M., Costa, T., Rocha, O., Spinelli, J. E., Cheung, N., & Garcia, A. (2015). Interconnection of thermal parameters, microstructure, and mechanical properties in directionally solidified Sn–Sb lead-free solder alloys. *Materials Characterization*, *106*, 52–61. https://doi.org/https://doi.org/10.1016/j.matchar.2015.05.015

Ebrahim Nataj, Z., Kazemi, A. S., & Abdi, Y. (2021). Surface effects and wettability measurement considerations in fluorinated carbon nanotubes. *Applied Physics A, 127*(11), 874. https://doi.org/10.1007/s00339-021-05029-z

Engwa, G. A., Ferdinand, P. U., Nwalo, F. N., & Unachukwu, M. N. (2019). Mechanism and Health Effects of Heavy Metal Toxicity in Humans. In O. Karcioglu & B. Arslan (Eds.), *Poisoning in the Modern World*. IntechOpen. https://doi.org/10.5772/intechopen.82511

Gan, K. F., & Ngan, A. H. W. (2018). The unusual size effect of eutectic Sn/Pb alloys in the micro regime: Experiments and modeling. *Acta Materialia*, *151*, 282–292. https://doi.org/https://doi.org/10.1016/j.actamat.2018.04.005

Hebbar, R. S., Isloor, A. M., & Ismail, A. F. (2017). Chapter 12 - Contact Angle Measurements. In N. Hilal, A. F. Ismail, T. Matsuura, & D. Oatley-Radcliffe (Eds.), *Membrane Characterization* (pp. 219–255). Elsevier. https://doi.org/https://doi.org/10.1016/B978-0-444-63776-5.00012-7

Jaffery, S. H. A., Sabri, M. F. M., Rozali, S., Hasan, S. W., Mahdavifard, M. H., AL-Zubiady, D. A. S., &Ravuri, B. R. (2022). Oxidation and wetting characteristics of lead-free Sn-0.7Cu solder alloys with the addition of Fe and Bi. *Microelectronics Reliability*, *139*, 114802. https://doi.org/https://doi.org/10.1016/j.microrel.2022.114802

Jiang, N., Zhang, L., Liu, Z.-Q., Sun, L., Long, W.-M., He, P., Xiong, M.-Y., & Zhao, M. (2019). Reliability issues of lead-free solder joints in electronic devices. *Science and Technology of Advanced Materials*, *20*(1), 876–901. https://doi.org/10.1080/14686996.2019.1640072

Kuang, H., Wu, B., Wang, J., Fu, J., Feng, Y., Yu, C., Wang, Z., Zhang, J., & Ji, Y. (2022). Wettability and thermal contact resistance of thermal interface material composited by gallium-based liquid metal on copper foam. *International Journal of Heat and Mass Transfer*, *199*, 123444. https://doi.org/https://doi.org/10.1016/j.ijheatmasstransfer.2022.123444

Li, Y., Chen, C., Yi, R., & Ouyang, Y. (2020). Review: Special brazing and soldering. *Journal of Manufacturing Processes*, *60*, 608–635. https://doi.org/https://doi.org/10.1016/j.jmapro.2020.10.049

Liu, G., Du, K., & Wang, K. (2016). Surface wettability of TiO2 nanotube arrays prepared by electrochemical anodization. *Applied Surface Science*, 388, 313–320. https://doi.org/10.1016/j.apsusc.2016.01.010

Niu, C., Dong, M., &Niu, Y. (2023). Lead toxicity and potential therapeutic effect of plant-derived polyphenols. *Phytomedicine*, *114*, 154789. https://doi.org/https://doi.org/10.1016/j.phymed.2023.154789

Patil, P. S., & Dabade, U. A. (2019). Selection of bearing material to comply RoHS regulations as per EU directive: A review. *Materials Today: Proceedings*, *19*, 528–531. https://doi.org/https://doi.org/10.1016/j.matpr.2019.07.648

Pecht, M., Shibutani, T., & Wu, L. (2016). A reliability assessment guide for the transition planning to lead-free electronics for companies whose products are RoHS exempted or excluded. *MicroelectronicsReliability*, *62*, 113–123. https://doi.org/10.1016/j.microrel.2016.03.020

Pivinskii, Y. E. (2021). Cement-Free Refractory Concretes. Part 7. Concrete Mix Properties and their Grain Size Distribution. *Refract Ind Ceram* *62*, 32–40. https://doi.org/10.1007/s11148-021-00556-x

Rocha, O. L., Costa, T. A., Dias, M., & Garcia, A. (2018). Cellular/dendritic transition, dendritic growth, and microhardness in directionally solidified monophasic Sn-2%Sb alloy. *Transactions of Nonferrous Metals Society of China*, *28*(8), 1679–1686. https://doi.org/10.1016/S1003-6326(18)64811-3

Sehirli, E., Erer, A. M., &Turan, M. K. (2022). A new approach for measuring the wetting angles of lead-free solder alloys from digital images. *Engineering Science and Technology, an International Journal*, *36*, 101279. https://doi.org/https://doi.org/10.1016/j.jestch.2022.101279

Šuryová, D., Kostolný, I., &Koleňák, R. (2020). Properties and application of Zn-based solders. *International Journal of Scientific and Technical Research in Engineering (IJSTRE) Www.Ijstre.Com*, *5*. www.ijstre.com

Thomas, O., leBot, B., Verrey, D., Durand, S., Harpet, C., Froment, A., &Jégou, B. (2022). High lead level in the Alps in XIXth century, learning from the analysis of 138 historical hair stands. *Chemosphere*, *286*, 131658. https://doi.org/https://doi.org/10.1016/j.chemosphere.2021.131658

Wernicki, E., Shu, Y., Fratto, E., Gao, F., Morose, G., Lucas, B., Yang, Z., &Gu, Z. (2023). Preparation and characterization of nano-solder paste with high nanoparticle loading and their thermal and printing properties. *Materials Chemistry and Physics*, *297*, 127399. https://doi.org/https://doi.org/10.1016/j.matchemphys.2023.127399

Zhou, Z., Chen, J., Yu, C., Wang, Y., & Zhang, Y. (2023). Failure Analysis of Printed Circuit Board Solder Joint under Thermal Shock. *Coatings*, *13*(3). https://doi.org/10.3390/coatings13030572